XVIII IMEKO WORLD CONGRESS
Metrology for a Sustainable Development
September, 17 – 22, 2006, Rio de Janeiro, Brazil

Current Developments in the Field of Shock Calibration

Th. Bruns [1], *A. Link* [2], *C. Elster* [3]

[1] Physikalisch-Technische Bundesanstalt, Braunschweig, Germany, thomas.bruns@ptb.de
[2] Physikalisch-Technische Bundesanstalt, Berlin, Germany, alfred.link@ptb.de
[3] Physikalisch-Technische Bundesanstalt, Berlin, Germany, clemens.elster@ptb.de

Abstract: Shock calibration is a major concern for a variety of mechanical applications. Examples of affected measurands are acceleration, force or torque. However, only for acceleration a written standard is available [1,2]. This text discusses the problems which need to be addressed in order to disseminate the respective units for shock applications or to improve the current standard for acceleration and proposes a promising approach to solve them.

Keywords: shock calibration, transfer function, parameter identification, modelling .

1 BASIC INFORMATION

Shocks and other transient signals are measured on large scale in a variety of sensor applications throughout the industry. In order to respond to the respective need for traceability the Physikalisch - Technische Bundesanstalt (PTB), as the German National Metrology Institute, has developed and setup different shock calibration facilities. A prominent position in this field is taken by the facilities for shock calibration of accelerometers, which are already in service for several years now. This is mainly due to the fact that acceleration is a key measurand for dynamic applications and that an international standard is already available since 1993 [1] (major revision in 2001 [2]).

In addition to the field of acceleration PTB has setup a facility for impact-force calibration, which might be considered as a related quantity to acceleration to some extent. However, as will be shown, the situation for the measurand force becomes even more complicated than the task of shock acceleration calibration, which in turn still bears some scientific challenges.

For an introduction the mentioned challenges are described in the following for the case of the shock acceleration calibration facilities of the PTB. Especially in order to generate high intensity shocks of peak values up to 10^5 m/s² a device based on the propagation of elastic waves in thin metal rods, the Hopkinson bar was constructed and further developed (cf. Fig. 1). Traceability is provided by the use of a heterodyne He-Ne Laser interferometer with a digital quadrature analysis of the Doppler-induced optical phase shift. Thus the determination of the input acceleration is based on the Laser wavelength (632,81 nm) and a precise time or frequency measurement.

According to the applicable international standards [2] the transducer's shock sensitivity modulus is defined as the ratio of the peak values of the output voltage of the transducer under test and the input acceleration. In order to calculate the input acceleration different methods are applicable. For both signals some suitable analogue filtering for the elimination of alias frequencies is mandatory. In addition digital low pass filters are suggested in order to get a “smooth” acceleration signal without high frequency distortion. In real application the cut off frequency of this low pass filters is typically set in the range of 10 kHz to 20 kHz.

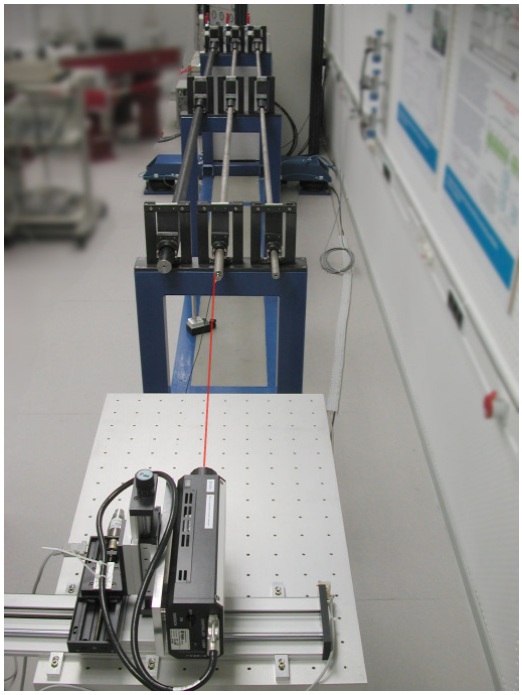

Fig. 1: Shock acceleration standard calibration device of PTB (5 km/s² to 100 km/s²)

During a linearity test with increasing intensities of acceleration in the range of 10^4 m/s² to 10^5 m/s² many accelerometers exhibit a systematic increase of the shock sensitivity S_{sh}. This behaviour, which might be understood in terms of some non-linearity of the accelerometer, needs a

deeper investigation for both correct understanding and appropriate handling. Additional problems arise when the shock calibrated transducer is used as a means of dissemination of the unit [3].

The phenomenon is demonstrated with the data of a shock calibration performed with the high intensity shock calibration facility of PTB, which is shown in Fig. 1.

For the sensitivity parameter S_{sh} defined by the mentioned international standard [2] the increase for the accelerometer chosen for this example increases by approx. 1,5 % over the whole range of intensities as depicted Fig. 2.

From calibration with sinusoidal acceleration the complex sensitivity (modulus and phase delay) are well known up to a frequency of 20 kHz from excessive investigations with PTB's high frequency standard calibration device. Linearity test at different frequencies with sinusoidal excitation revealed no non-linearity, for high quality accelerometers.

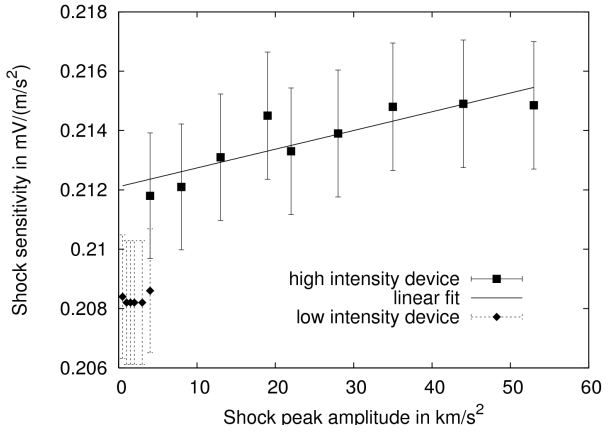

Fig. 2: Shock sensitivity according to [2] for different intensities measured on two different standard devices with different working principles.

The nature of this phenomenon is understood as soon as not only the intensity of the shock acceleration is considered but the duration and signal shape are taken into account as well.

A qualitative explanation is given by the decreasing pulse duration of the shock signal with increasing intensity. Due to non-linear effects in the shock generation process, which are present in all known high intensity shock devices, the impulse duration decreases with increasing shock intensity. With regard to the frequency contents, i.e. considered in the frequency domain, this leads to a broader spectrum with higher frequencies included for shorter impulses. Since the sinusoidal sensitivity of an accelerometer is generally increasing for higher frequencies the response of the accelerometer for shorter shocks is also increasing. For the ratio of the peak values, which defines the shock sensitivity S_{sh} this results in the observed behaviour.

In the following sections this qualitative explanation is described in more detail on the basis of a simple dynamical model. The goal is to provide a basic route for the description of the problem which can lead to enhanced calibration procedures.

2 MODELING OF ACCELEROMETERS

The dynamic system considered as a representation of an accelerometer is a linear single mass oscillator with constant stiffness and damping (c.f. Fig. 3). The damping is proportional to the velocity.

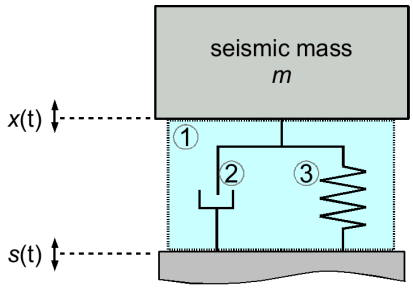

Fig. 3: Graphical display of the model of an accelerometer used for the parameter identification. The sensing element (1) is representated with constant damping (2) and stiffness (3)

The equation of motion of this system is given by

$$m\ddot{x} + c(\dot{x} - \dot{s}) + k(x - s) = 0\ . \tag{1}$$

Equation (1) describes the dynamics of the seismic mass $x(t)$ given the displacement $s(t)$ of the base and its velocity $\mathrm{d}s(t)/\mathrm{d}t$. This motion of the base exerts a force on the seismic mass m via a spring element with stiffness k and damping coefficient c. For e.g. a piezo-electric transducer the output charge is proportional to x(t)-s(t). From (1) immediately

$$m(\ddot{x} - \ddot{s}) + c(\dot{x} - \dot{s}) + k(x - s) = -m\ddot{s}\ , \tag{2}$$

follows. Hence, substituting (x-s) by y then yields the relation

$$\ddot{y} + 2\delta\omega_0\dot{y} + \omega_0^2 y = \rho a \tag{3}$$

where $a = -\ddot{s}$ is the acceleration of the base. The parameters δ, ω_0, ρ denote damping, resonant frequency and transformation constant of the input acceleration a. The physical model (1) thus leads to the model (3) which describes how the output voltage of the transducer (which is proportional to $y(t)$) is related to the applied acceleration $a(t)$ of the transducer. Note that in a calibration experiment the acceleration $a(t)$ of the accelerometer is measured with the help of an interferometer as described in the introduction.

The complex sensitivity

$$H(\omega) = \frac{\rho}{(\omega_0^2 - \omega^2) + 2j\delta\omega\omega_0}\ . \tag{4}$$

is the complex frequency response of the linear time invariant system (3) and it describes the frequency response of the output voltage to an applied acceleration. Magnitude and phase response of the system are plotted in Fig. 4 for a resonance frequency of f_0 = 50 kHz and δ = 0,06.

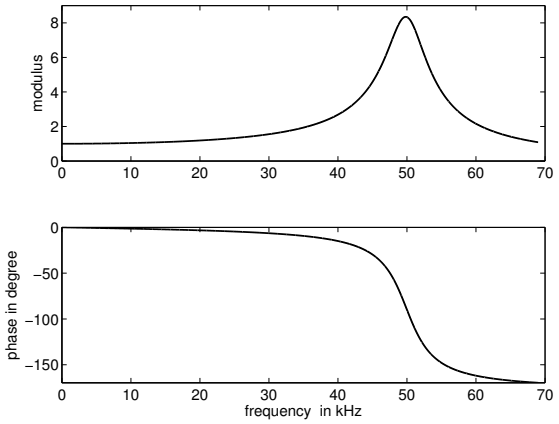

Fig. 4: Magnitude (top) and phase (bottom) response of the model according to Eq. 4. (f_0 = 50 kHz, δ = 0,06)

The increase of the magnitude of the sensitivity towards higher frequencies (below the resonance frequency f_0) is clearly visible. As a consequence, different shock excitations with different spectral contents can lead to different shock sensitivities. In particular, a shock with an increased spectrum in the large frequency range will result in an increased shock sensitivity. The indicated 'non-linearity' in Fig. 2 thus might also be simply due to the fact that the different shocks were of different spectral contents, as the simulations in the next section will demonstrate.

3 THE RESPONSE OF THE MODEL ACCELEROMETER

The properties of the accelerometer model of the previous section shall now be analyzed under shock load. In particular, it is shown that this model predicts the behaviour observed in Fig. 2. That is, by applying shock accelerations of different intensities and different duration (therefore different spectral contents) the ratios of the (modelled) output voltage peak and the applied input acceleration peak differ for the same accelerometer (i.e. chosen model parameters in (3)).

Fig. 5 shows the different input shock accelerations considered with different frequency contents. Each of these shocks can be characterized by an individual centre frequency f_{imp} and impulse duration τ. For these input shock accelerations model (3) was solved for the output voltage using the model parameters f_0 = 50 kHz, $\rho/(2\pi f_0) = 1$ and different damping factors taken from the range $\delta = 0.01, \ldots, 0.3$. This solution was based on an appropriate discretization of (3) leading to a recursive filter [4]. For each input acceleration shock then the ratio of the calculated output voltage peak and the input acceleration peak was calculated. For decreasing f_{imp} this ratio approaches the value of $\rho/(2\pi f_0) = 1$. Fig. 6 shows the deviation of these ratios from the shock sensitivity $S_{\mathrm{Sh}} = 1$ for the different input acceleration shocks, the so called dynamical error. Just as for the measurement results shown in Fig. 2 here also different shock sensitivities result for the same (model of an) accelerometer. Hence, the simple model (3) already accounts for the fact that different input acceleration shocks can lead to different shock sensitivities.

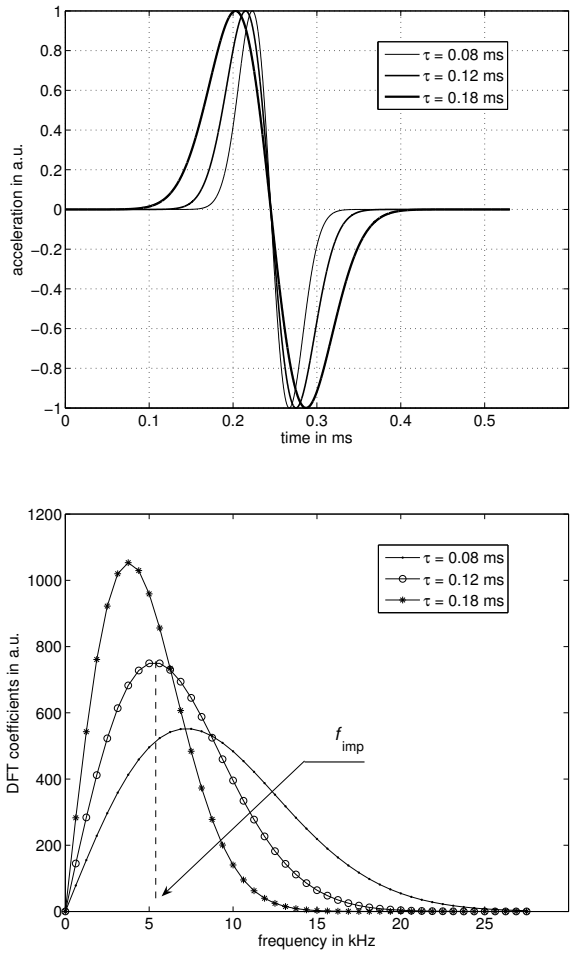

Fig. 5: Different input shock acceleration curves (top) with different frequency contents (bottom).

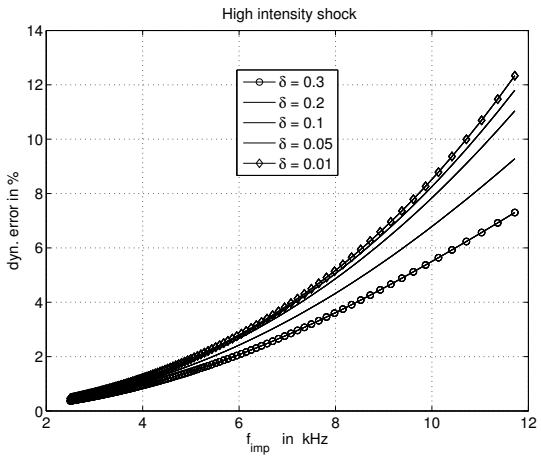

Fig. 6: Magnitude (top) and phase (bottom) response of the model according to Eq. 4. (f_0 = 50 kHz, δ = 0,06)

Different shock sensitivities thus reflect not necessarily some inherent non-linearities but can be due to the different spectral contents of the applied acceleration shocks.

Consequently, shock sensitivities do not uniquely characterize an accelerometer but depend on the actual shock being applied.

The proposed model (3) allows the observed behaviour in Fig. 2 to be explained. In the following section it is shown that this model also allows a precise quantitative description of the accelerometer's behaviour and hence can be used for an appropriate analysis of shock calibration measurements.

4 A SOLUTION FOR ACCELEROMETERS

Elaborate investigations of the PTB strongly suggest that a better solution for the description of the accelerometer is found by modelling. The corner stone for this is already given with Eq. (3). If it is in fact possible to model an accelerometer by an ordinary differential equation like (3) then the complex sensitivity can be described by a small set of parameters (i.e. δ, ω_0, ρ). The general advantages of this approach are imminent. It will be possible to predict the response of the transducer for arbitrary signals, therefore the results obtained from calibration data are generally valid for arbitrary applications, while today's methods provide calibration results in a strict sense either for shock or for sinusoidal signals.

The questions at this point are

1. Is this description valid?
2. If yes, how can the parameters be identified?
3. What happens to measurement uncertainty?

For two different accelerometer types of back-to-back design these questions have been answered recently [5]. It was shown that the behaviour of the respective accelerometers can be described effectively by the model (3). For that purpose a parameter identification procedure based on a linear least-squares approach in the frequency domain was developed. Based on the calculated parameter sets the complex sensitivity (magnitude and phase) was calculated from the model description for both transducers in a frequency range from 40 Hz to 20 kHz. The associated uncertainties of the model parameters were determined by Monte-Carlo methods. The resulting frequency dependency of the complex sensitivity (calculated by model-based shock data analysis) was then compared with sinusoidal calibration data of the identical transducers measured according to [6] on the High Frequency Standard Calibration Facility of the PTB.

The outcome of this validation procedure is shown graphically in Fig. 7. The complex sensitivity calculated from the shock data is in very good agreement with the calibration data determined in accordance to international standards for sinusoidal calibration.

Thus all three questions above can be regarded as answered with a valid solution for the underlying problem. The applied model is valid and in addition allows now for the prediction of the input-output behaviour of the utilized accelerometers for arbitrary signals, even beyond the sinusoidal or shock signals used for this investigation.

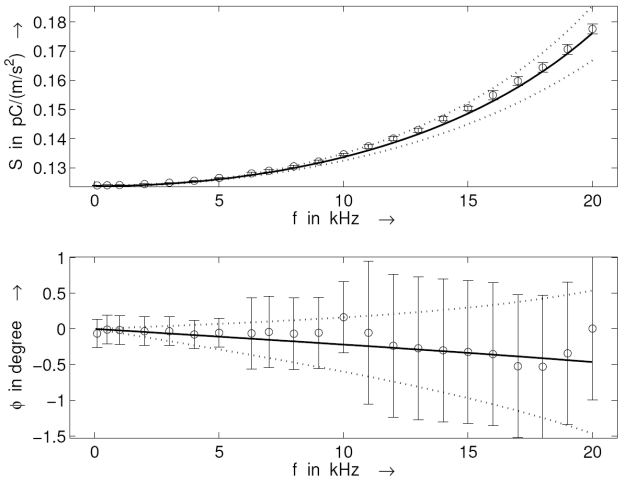

Fig. 7: Complex sensitivity as a function of frequency (*f*) of the accelerometer 8305 determined from single shock (solid and dashed) and sinusoidal excitations (error bar plot). Top: amplitude response, bottom: phase response. The range of associated uncertainties (coverage factor *k*=2) are marked by dotted lines and bars, respectively

5 CALIBRATION APPROACH FOR FORCE TRANSDUCERS

The dynamic behaviour of a force transducer excited by impulse forces depends on the construction of the force transducer, the impact mass and the loading mass, and the mechanic coupling of all connected masses. Therefore, the sensitivity of the transducer reflects the measurement structure of the calibration device and can only be determined for the given structure of the calibration setup. Recently, a new calibration device has been developed at the PTB [7]. It will provide traceability for the generated force via the base units of mass and acceleration (c.f. Fig. 8). The force pulse is generated by the central collinear impact of two steel cubes, with the transducer placed between them. By measuring the velocity of the loading mass, it is possible to calculate its acceleration and thus to calculate the force acting on the transducer.

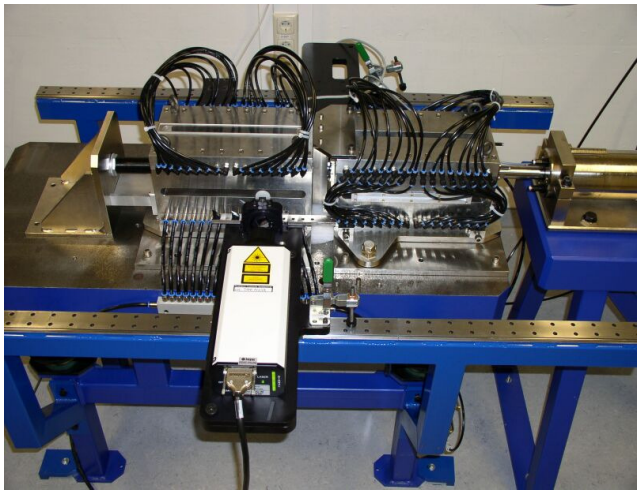

Fig. 8: Impact force standard measuring device of PTB.

The force then can be compared to the electric response of the transducer in order to determine the sensitivity of the transducer. To analyse the influence of the calibration setup on the obtained sensitivity the mass spring system of calibration system has been modelled.

5.1 The Model

The model (c.f. Fig. 9 and [8]) consists of four mass bodies and three visco- elastic coupling springs. From left to right: the impactor mass m_1 hits with its impact velocity the force introduction parts of the transducer. The contact is a non-linear pressure only transmitting spring, because the transducer's head surface has a spherical shape. The coupling is quantified by the elastic constant S_{1h} and the damping constant γ_{1h}. The transducer under test is modelled by the two masses m_h (head mass) and m_b (base mass) coupled by a bidirectional linear spring with the elastic spring constant S_{hb} and the damping constant γ_{hb}.

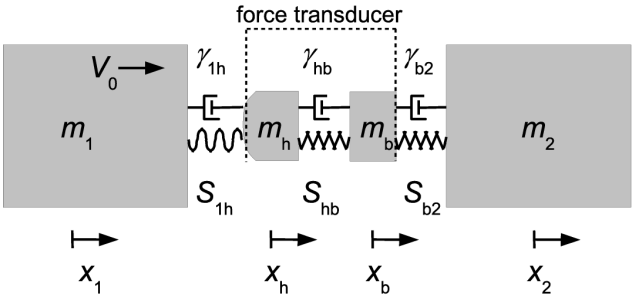

Fig. 9: Mass spring model for calibration of force transducers

Finally the base mass of the transducer is fixed on the second mass m_2 of the calibration device. The finite stiffness of the fixation is taken into account by an additional linear spring with the constants S_{b2} and γ_{b2} respectively. The dynamic behaviour of the model is described by the system of ordinary differential equations (SODE):

$$\ddot{x}_1 = -\frac{S_{1h}}{m_1}(x_1 - x_h)^{3/2} H(x_1 - x_h) - \frac{\gamma_{1h}}{m_1}(\dot{x}_1 - \dot{x}_h) H(x_1 - x_h),$$

$$\ddot{x}_h = +\frac{S_{1h}}{m_h}(x_1 - x_h)^{3/2} H(x_1 - x_h) - \frac{S_{hb}}{m_h}(x_h - x_b) + \frac{\gamma_{1h}}{m_h}(\dot{x}_1 - \dot{x}_h) H(x_1 - x_h) - \frac{\gamma_{hb}}{m_h}(\dot{x}_h - \dot{x}_b),$$

$$\ddot{x}_b = +\frac{S_{hb}}{m_b}(x_h - x_b) - \frac{S_{b2}}{m_b}(x_b - x_2) + \frac{\gamma_{hb}}{m_b}(\dot{x}_h - \dot{x}_b) - \frac{\gamma_{b2}}{m_b}(\dot{x}_b - \dot{x}_2),$$

$$\ddot{x}_2 = +\frac{S_{b2}}{m_2}(x_b - x_2) + \frac{\gamma_{b2}}{m_2}(\dot{x}_b - \dot{x}_2). \qquad (5)$$

$H(x)$ denotes the Heavyside function

$$H(x) = \begin{cases} 0, & x < 0 \\ 1, & otherwise \end{cases} \qquad (6)$$

used to model the pressure coupling only between m_1 and the transducer namely m_h. The calibration system is excited by the driving force $F_1(t) = m_1 \ddot{x}_1(t)$. For a given initial velocity $v_0 = \dot{x}_1(t = 0)$ of m_1 a impulse-like driving force is generated and transmitted via the force transducer onto the mass m_2.

The transducer's electric response is assumed to be proportional to the displacement difference x_h-x_b. The mass m_2 to which the transducer is mounted is excited by the acceleration $a_2 = \ddot{x}_2$. Therefore the transducer's response upon a force impulse, i.e. its sensitivity, is defined by

$$S_{ShF}(f) = \frac{\chi \cdot \left(X_h(f) - X_b(f)\right)}{m_2 \cdot A_2(f)}, \qquad (7)$$

in the frequency domain, where capital letters denote the Fourier components of corresponding signals at frequency f and χ is a transducer constant transforming the sensed displacement difference into a force signal.

5.2 Model evaluation

The usefulness of the model is evaluated by comparing simulation and experimental results. The measurements were obtained from a force measuring device which consists of a force transducer with the mounted loading mass $m_2 = 9{,}8815$ kg. For force generation, the mass $m_1 = 10{,}1126$ kg is decelerated.

The velocity of both the m_1 and m_2 masses has been measured using laser interferometry. In addition to these measurements, the transducer's electrical signal was recorded from the charge amplifier output.

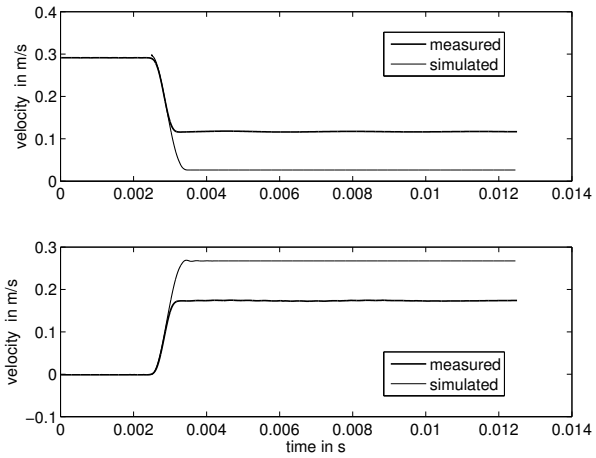

Fig. 10: Measured and simulated velocities of the masses m_1 and m_2.

The simulation results are obtained by solving the nonlinear system of differential equations with the measured velocity as initial value. For the chosen values of model parameters

$m_h = 0.152$ kg,

$m_b = 0.124$ kg,

$S_{1h} = 5.028 \cdot 10^{10}$ N/m$^{3/2}$,
$S_{hb} = 7{,}682 \cdot 10^{7}$ N/m,
$S_{b2} = 6{,}844 \cdot 10^{9}$ N/m,
$\gamma_{1h} = 7{,}936 \cdot 10^{2}$ N/(m/s),
$\gamma_{hb} = 3.325 \cdot 10^{3}$ N/(m/s)
and
$\gamma_{b2} = 2.089 \cdot 10^{2}$ N/(m/s)
the simulation results appear to be qualitatively in a good agreement with the measurements results.

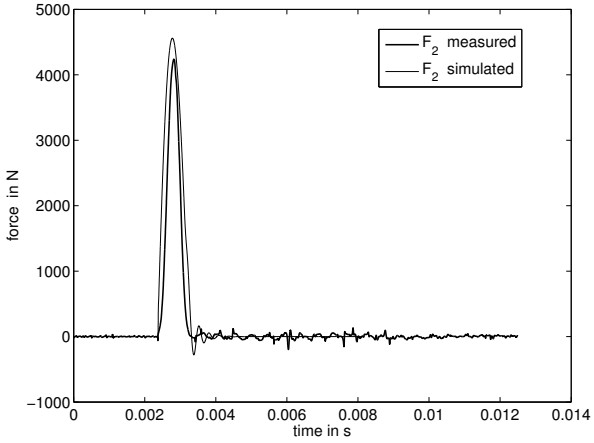

Fig. 11: Measured and simulated force acting on the mass m_2.

Figures 10 and 11 show the measured and simulated velocities of the masses m_1 and m_2, and the measured and simulated force signals acting on m_2. Larger deviations between measured and simulated velocity signals occur for the time interval where the formation of the force impulse has been finished, whereas the measured and simulated force impulses appear to be in good agreement.

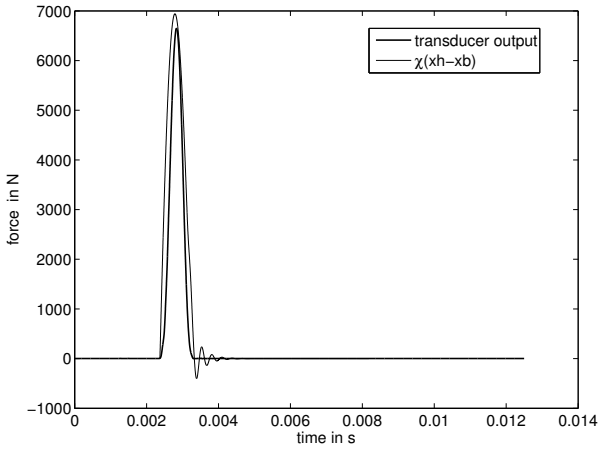

Fig. 12: Comparison of the measured transducer output with the scaled displacement difference (deformation)..

Fig. 12 allows to compare the measured transducer output signal with the simulated difference x_h-x_b multiplied by an arbitrarily chosen constant χ in order to account for the transducer transformation of deformation into force. Finally, Fig 13 displays the measured and simulated modulus of the complex sensitivity S_{ShF} (c.f. Eq. (7)) using the same transformation constant for the difference signal x_h-x_b. In Fig. 13, the simulated sensitivity curve demonstrates the possibility of the proposed impulse generation to cover a broad frequency range. Observed deviations between the measured and simulated sensitivities at single frequencies give rise to further analysis of the calibration setup in particular with respect to the force introduction.

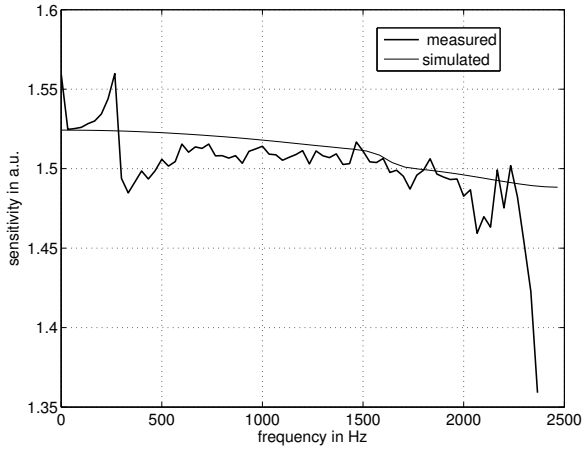

Fig. 13: Comparison of the measured Sensitivity S_{ShF} with the respective sensitivity calculated from the model.

Overall, the model allows to explain impulse formation on the masses m_1 and m_2 and the deformation or displacement difference x_h-x_b. To describe the detected deviation between simulated and measured velocities after formation of the force impulses, refinements of the proposed model should be considered. Nevertheless, the proposed model structure seems to be appropriate for describing the dynamic behaviour of a force measuring device and justifies the frequency response estimate (7).

6 SUMMARY AND CONCLUSION

Current developments in the field of shock calibration have been presented. For accelerometers, shock sensitivities are currently determined as the ratio of the output voltage peak and the peak value of the applied shock acceleration. The drawback of this procedure is that such sensitivities do not uniquely characterize an accelerometer but depend on the particular shock acceleration applied. A recently developed approach was described which overcomes these shortcomings. The approach is based on an ordinary second order differential equation model. It allows a unique characterization of the accelerometer by shock calibration and hence can improve current standards.

Analysis of shock calibration measurements of force transducers appears to be more complicated. The reason is the two-sided coupling between the calibration facility and the transducers which must be taken into account. As a consequence, modelling the behaviour of a force transducer leads to a non-linear differential equation which complicates parameter estimation and the determination of the

uncertainty associated with the applied model. A particular model was proposed and first results show that this model describes the behaviour of the force transducer qualitatively correct. Future research will address the refinement of the model and the development of robust identification procedures. In addition, quantitative model validation shall be carried out.

The results presented here for the proposed procedures in the analysis of shock calibrations are encouraging and they demonstrate that the limits of current standards on shock calibration can be overcome. It is concluded that the proposed procedures should serve as a basis for future written standards on shock calibration.

REFERENCES

[1] ISO 5347-10 "Methods for the calibration of vibration and shock pick-ups – Part 10 Primary calibration by high impact shocks", Geneva 1993 (out of date).

[2] ISO 16063-13: 2001 "Methods for the calibration of vibration and shock transducers -- Part 13: Primary shock calibration using laser interferometry", Geneva, 2001

[3] ISO 16063-22: 2005 "Methods for the calibration of vibration and shock transducers – Part 22: Shock calibration by comparison to a reference transducer", Geneva, 2005

[4] A. Link, W. Wabinski, H.-J. v. Martens, "Accelerometer identification by high shock intensities using laser interferometry", Proc. of SPIE Vol. 5503, Ancona 2004

[5] A. Link, A Täubner, W. Wabinski, Th. Bruns, C. Elster, (2006), "Calibration of accelerometers: Determination of amplitude and phase response upon shock excitation", submitted to Measurement Science and Technology

[6] ISO 16063-11: 1999 "Methods for the calibration of vibration and shock transducers – Part 11: Vibration calibration by laser interferometry", Geneva, 1999

[7] M. Kobusch, Th. Bruns, "The New Impact Force Machine at PTB", Proc. of XVII IMEKO World Congress, Dubrovnik (Croatia), 2003

[8] Th. Bruns, R. Kumme, M. Kobusch, M. Peters, "From oscillation to impact: The design of a new force calibration device at PTB", Measurement, 32, (2002), 85-92